

# Change in Radius of Gyration of Semicrystalline Polymers upon Crystallization

Marc L. Mansfield\*

Engineering Materials Program, Department of Chemical and Nuclear Engineering,  
University of Maryland, College Park, Maryland 20742. Received March 18, 1985

**ABSTRACT:** The gambler's ruin model of semicrystalline polymer chains predicts a radius of gyration proportional to the square root of the molecular weight and gives  $2x_a/3 + 1/3x_a$  for the ratio of semicrystalline to molten characteristic ratios, where  $x_a$  is the amorphous fraction. This value is near unity for  $x_a$  in the usual experimental range, consistent with SANS results on the majority of semicrystalline polymers. Tilting of the polymer axis relative to the lamellar plane affects the characteristic ratio, but not strongly. The end-to-end vector follows an anisotropic Gaussian distribution elongated normal to the lamellar plane.

## Introduction

Over the past several years, as a result of small-angle neutron scattering studies, it has become apparent that semicrystalline polymer chains obey Gaussian statistics, with root mean square gyration radii obeying

$$R_g = AM^{1/2} \quad (1)$$

for  $M$  the molecular weight.<sup>1-5</sup> (Some exceptions<sup>6</sup> have been observed; nevertheless, eq 1 is followed in the majority of cases.) Even more surprising has been the observation that the prefactor,  $A$ , is close to its value in the melt.<sup>1-5</sup> Clearly, this behavior relates to the nature of the crystal-amorphous interface in semicrystalline polymers and has often been taken as evidence for a large amount of irregular or nonadjacent reentry in such crystals.

Guttman, DiMarzio, and Hoffman<sup>7,8</sup> have argued that the fraction of near-adjacent reentry in melt-crystallized, lamellar systems is at least  $1 - K(\sec \theta)/3$  for  $\theta$  the tilt angle (the angle that the crystal axis makes with the direction normal to the lamellar plane) and for  $K = (\rho_a/\rho_c)(l_b/l_u)$ , a constant near 1. (Here  $\rho_a$  and  $\rho_c$  are amorphous and crystalline densities;  $l_b$  and  $l_u$  are the bond length and its projection on the crystal axis, respectively.) They modeled chains in the amorphous domain as random walks between two absorbing barriers (the so-called gambler's ruin problem). The gambler's ruin limit on the amount of random reentry derives from the fact that random walks between two barriers are too long to permit one such walk from each crystalline stem. For example, for  $K$  near 1 and  $\theta$  near 0, gambler's ruin predicts at least  $2/3$  near-adjacent reentry, with  $2/3$  of the crystalline stems returning very near (within a few unit cells) their exit point. The remaining  $1/3$  perform random walks in the amorphous domain, terminating either in the same crystallite (forming a loop) or the neighboring crystallite (forming a tie). When only  $1/3$  random reentry is allowed, an amorphous density near that of the crystal is guaranteed.

This result has since been verified in Monte Carlo calculations<sup>9</sup> incorporating a partially ordered interfacial layer and in related, mean-field calculations.<sup>10,11</sup> The purpose of this paper is to demonstrate that the view of semicrystalline morphology provided by the gambler's ruin calculation is consistent with a liquid-like radius of gyration.

That such chains exhibit Gaussian statistics should not be surprising. Gaussian behavior is exhibited whenever the bond correlations  $\langle \cos \theta_{ij} \rangle$  are 0 for  $|j - i|$  sufficiently large, where  $\theta_{ij}$  is the angle between bonds  $i$  and  $j$ . In flexible,  $\theta$ -state chains, such bond correlations decay very

rapidly. In semicrystalline polymers with  $1/3$  random reentry, these correlations undoubtedly extend over several hundred bonds, but they too must eventually dissipate. In both cases, sufficiently long chains exhibit Gaussian statistics. Departures from ideality at lower molecular weights can be expected in semicrystalline polymers. Such departures have, in fact, been observed.<sup>12</sup>

Of course, it is one thing to successfully predict the exponent in eq 1 and entirely another to predict the prefactor. However, Guttman et al.<sup>13</sup> were able to do this, employing a rotational isomeric-state polyethylene model, solved by Monte Carlo techniques. They obtained unperturbed dimensions close to those of the melt using a model with a relatively large amount of adjacent reentry and with random reentry sufficient to fill the amorphous domains. In this paper, we obtain a similar result, in the form of a very simple equation relating the ratio of semicrystalline and molten characteristic ratios to the degree of crystallinity. Our formulas are consistent with the gambler's ruin<sup>7,8</sup> result that  $2/3$  of the emergent stems return to the same lamella at neighboring sites (within one or two unit cells) and the remaining  $1/3$  enter the amorphous region, performing random walks before returning to one or the other of the two neighboring lamellae. The result is a surprisingly simple equation, eq 20, relating the ratio of semicrystalline to molten characteristic ratios to the degree of crystallinity, predicting that the characteristic ratio is always within 10% of the molten characteristic ratio for crystallinities below 60%. In the quench-crystallized samples most often examined by neutron scattering, crystallinities almost always lie within that range.

The lack of long range correlation in bond vectors, although sufficient to give Gaussian behavior, does not necessarily imply spherical symmetry. Suppose that the drunken sailor, the celebrated random walker, takes twice as many steps to the north or south than to the east or west. His mean-square displacement is still proportional to the total number of steps, and his probability distribution is still Gaussian, but loci of constant probability are concentric ellipses, not circles. The present model of semicrystalline polymers exhibits similar behavior. Although low-order correlations such as  $\langle \cos \theta_{ij} \rangle$  decay along the chain, higher order ones, such as  $\langle P_2(\cos \theta_{ij}) \rangle$  persist, giving rise to anisotropy.

## Computation of the Characteristic Ratio without Tilt

Decompose the end-to-end vector of the chain into a set of vectors  $V_j$  (see Figure 1) such that each  $V_j$  extends from some particular point at which the chain enters a crystallite to the next point at which the chain again enters some crystallite. We need only consider four "states" of each  $V_j$ , as in Figure 2.  $L_+$  and  $T_+$  designate loops and ties with

\* Current address: Michigan Molecular Institute, Midland, MI 48640.

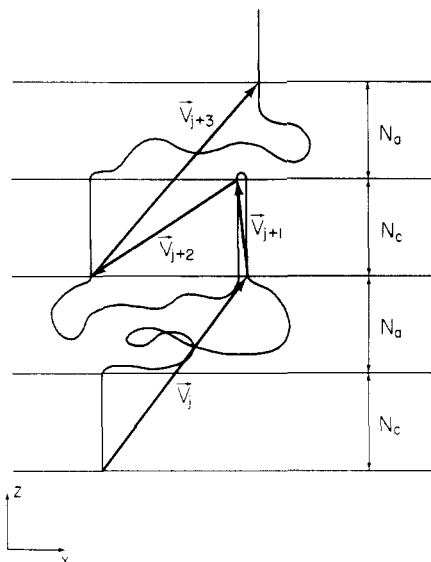


**Figure 1.** Schematic diagram of the present model, showing resolution of the end-to-end vector into a sequence of vectors,  $V_j$ .

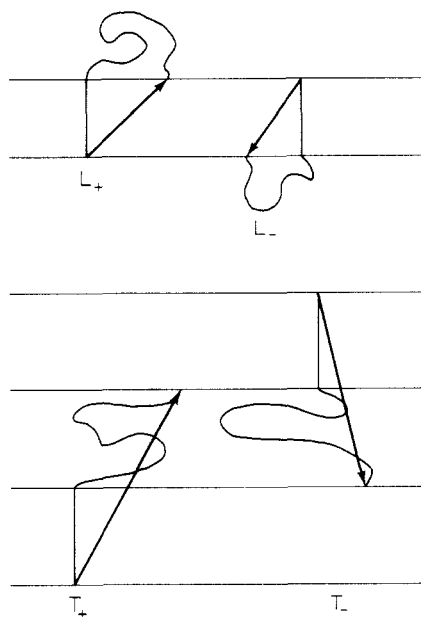


**Figure 2.** Admissible "states" of each vector,  $V_j$ , are up or down loops ( $L_{\pm}$ ) and up or down ties ( $T_{\pm}$ ).

positive  $z$ -projections, while  $L_-$  and  $T_-$  designate the same objects but with negative  $z$ -projections. We assume that loops and ties appear with probabilities  $\epsilon$  and  $\delta$ , respectively, with  $\delta + \epsilon = 1$ . Note that the object following a loop must have its sign reversed, while the object following a tie will have the same sign. In other words, only  $L_-$  or  $T_-$  can follow  $L_+$ , while only  $L_+$  or  $T_+$  can follow  $T_+$ .

Units are assumed such that the statistical segment length of the chain in the melt is unity, i.e., such that the mean-square end-to-end distance,  $\langle R^2 \rangle$ , is equal to  $N$ , the number of bonds.  $N_c$  and  $N_a$  are the thicknesses of the crystal and amorphous layers in these length units, respectively.  $N$  is the number of bonds in the chain, and  $n$  is the number of  $V$ -vectors into which the chain is resolved. We consider an ensemble in which  $n$ , rather than  $N$  is fixed, the distinction being unimportant as  $N \rightarrow \infty$ .<sup>14</sup>

For sufficiently long chains

$$\langle R^2 \rangle = n \sum_{j=-\infty}^{+\infty} \langle V_0 \cdot V_j \rangle \quad (2)$$

where for concreteness we may take  $V_0$  to be in the middle of the chain. The characteristic ratio is defined as

$$C_{\infty} = \langle R^2 \rangle / \langle N \rangle \quad (3)$$

Thus defined,  $C_{\infty} = 1$  in the melt. It follows that

$$C_{\infty} = (n / \langle N \rangle) [\langle V_0^2 \rangle + 2 \sum_{j=1}^{\infty} \langle V_0 \cdot V_j \rangle] \quad (4)$$

Assuming the same density in both phases, we obtain

$$\langle N \rangle = n(N_c + N_a) \quad (5)$$

and

$$\langle V_0^2 \rangle = \epsilon \langle x^2 + y^2 + z^2 \rangle_{\text{loop}} + \delta \langle x^2 + y^2 + z^2 \rangle_{\text{tie}} \quad (6)$$

where  $x$ ,  $y$ , and  $z$  are the components of  $V_0$  in a coordinate system in which  $z$  lies along the crystal axis. Therefore

$$\langle V_0^2 \rangle = \epsilon \langle x^2 + y^2 \rangle_{\text{loop}} + \delta \langle x^2 + y^2 \rangle_{\text{tie}} + \epsilon N_c^2 + \delta (N_a + N_c)^2 \quad (7)$$

Two thirds of the loops return to nearby sites in the lattice and have negligible  $x^2 + y^2$  values (relative to  $N_a$ ). Of the remaining third, the gambler's ruin result<sup>7</sup> is  $\langle x^2 + y^2 \rangle = 4N_a/3$ . Therefore

$$\langle x^2 + y^2 \rangle_{\text{loop}} = 4N_a/9 \quad (8)$$

includes contributions from both random and adjacent reentry. For ties, the gambler's ruin result<sup>7</sup> is

$$\langle x^2 + y^2 \rangle_{\text{tie}} = 2N_a^2/3 \quad (9)$$

In eq 8 and 9 we have consistently neglected terms of lower order in  $N_a$ . Equation 7 becomes

$$\langle V_0^2 \rangle = 4\epsilon N_a/9 + \epsilon N_c^2 + 2\delta N_a^2/3 + \delta (N_a + N_c)^2 \quad (10)$$

The sum in eq 4 can be computed with the usual generator matrix techniques.<sup>15</sup> We obtain

$$\langle V_0 \cdot V_j \rangle = [\epsilon N_c \delta (N_a + N_c)] \cdot T^j \cdot \begin{bmatrix} N_c \\ N_a + N_c \end{bmatrix} \quad (11)$$

$$T = \begin{bmatrix} -\epsilon & \delta \\ -\epsilon & \delta \end{bmatrix} \quad (12)$$

Raising  $T$  to the  $j$ th power generates statistical weights of all possible sequences of states between  $V_1$  and  $V_j$ ; the statistical weights of  $V_0$  appear in the row vector preceeding  $T^j$ . We are assuming that  $\langle V_0 \cdot V_j \rangle$  for each sequence of states is equal to the weight of that sequence times  $\pm N_c^2$ ,  $\pm (N_a + N_c)^2$ , or  $\pm N_c(N_a + N_c)$  depending on whether  $V_0$  and  $V_j$  are both loops, both ties, or one is a tie and the other is a loop. This explains the appearance of  $N_c$  and  $N_a$  terms in the row and column vectors and is equivalent to assuming that the amorphous runs of  $V_0$  and  $V_j$  are uncorrelated. The sign of  $\langle V_0 \cdot V_j \rangle$  depends of course on the number of intervening loops, since these reverse the orientation of the chain, and so  $-\epsilon$ , rather than  $\epsilon$ , is the appropriate entry for the first column of  $T$ .

Now factoring  $(N_a + N_c)^2$  out of eq 11 and performing the sum, we obtain

$$\sum_{j=1}^{\infty} \langle V_0 \cdot V_j \rangle = (N_a + N_c)^2 [\epsilon x_c \delta] \cdot Q \cdot \begin{bmatrix} x_c \\ 1 \end{bmatrix} \quad (13)$$

where

$$Q = T \cdot (1 - T)^{-1} \quad (14)$$

and

$$x_c = N_c / (N_a + N_c) \quad (15)$$

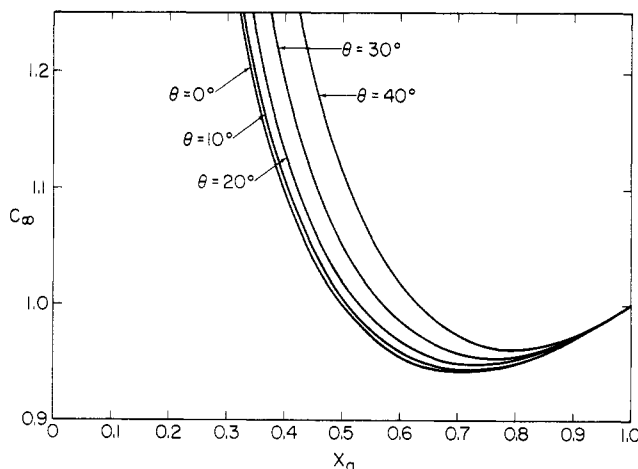


Figure 3. Characteristic ratio of the present model as a function of the amorphous fraction ( $x_a$ ) at the indicated tilt angles.

is the degree of crystallinity, neglecting density differences between the two phases. We find

$$Q = T/(2\epsilon) \quad (16)$$

or

$$C_\infty = (n/\langle N \rangle)[\langle V_0^2 \rangle + \epsilon^{-1}\langle \mathbf{V}_0 \cdot \mathbf{V}_1 \rangle] \quad (17)$$

while

$$\langle \mathbf{V}_0 \cdot \mathbf{V}_1 \rangle = (N_a + N_c)^2(\delta^2 - \epsilon^2 x_c^2) \quad (18)$$

Now, by combining eq 5, 10, 17, and 18 and rearranging, we obtain

$$C_\infty = 4\epsilon x_a/9 + 2\delta N_a x_a/3 + \delta(N_a + N_c)/\epsilon \quad (19)$$

for  $x_a = 1 - x_c$ , the amorphous fraction. One third of the V-vectors make nonadjacent runs through the amorphous domain; of these, gambler's ruin predicts that  $1/N_a$  are ties. Therefore  $\delta = (3N_a)^{-1}$ , and to leading order in  $N_a$ ,  $\epsilon = 1$ . Therefore, the final result for the characteristic ratio, to leading order in  $N_a$ , is

$$C_\infty = (2x_a + x_a^{-1})/3 \quad (20)$$

A plot of eq 20 appears in Figure 3. Note that in the molten limit, where  $x_a = 1$ ,  $C_\infty = 1$  as expected, so eq 20 also represents the ratio between semicrystalline and molten characteristic ratios in the general case for which  $C_\infty \neq 1$  in the melt. As  $x_a$  drops from 1, eq 20 also decreases, passing through a minimum at  $x_a = 2^{-1/2} = 0.707$ , at which time  $C_\infty = 2(2^{1/2})/3 = 0.943$ . At  $x_a = 0.5$ ,  $C_\infty = 1$ , and at  $x_a = 0.4$ ,  $C_\infty = 1.1$ . As  $x_a$  decreases further,  $C_\infty$  increases and diverges at  $x_a = 0$ . Therefore, for crystallinities below 60%, eq 20 predicts that the characteristic ratio will be within 10% of its value in the melt.

Each of the terms in eq 20 can be traced to terms in eq 10. The term  $2x_a/3$  results from the first and third terms on the right-hand side of eq 10, while the term  $(3x_a)^{-1}$  comes from the last term of eq 10. The two large terms  $N_c^2$  (from eq 10) and  $\epsilon^{-1}\langle \mathbf{V}_0 \cdot \mathbf{V}_1 \rangle$  (from eq 17) cancel one another and are absent from the final expression.

### Computation of the Characteristic Ratio with Tilt

Commonly, the polymer axis is tilted relative to the plane of the lamellae, as shown in Figure 4. Consequently, let us consider the case in which the polymer chains are inclined at an angle  $\theta$ , with  $x$  and  $z$  axes aligned as shown in Figure 4. As previously discussed,<sup>7,8</sup> the probability that

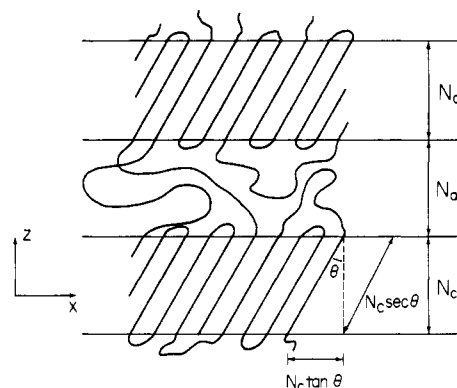


Figure 4. Schematic diagram of the model with tilt.

any given stem enters the amorphous domain is now  $(\sec \theta)/3$ , rather than  $1/3$ . Therefore,  $\delta = (\sec \theta)/3N_a$ , and<sup>16</sup>

$$\langle N \rangle = n(\sec \theta)(N_a + N_c) \quad (21)$$

In addition, we now have

$$\langle V_0^2 \rangle = N_c^2 \tan^2 \theta + (4\epsilon/9)N_a \sec \theta + \epsilon N_c^2 + (2\delta/3)N_a^2 + \delta(N_a + N_c)^2 \quad (22)$$

and

$$\langle \mathbf{V}_0 \cdot \mathbf{V}_j \rangle = [\epsilon N_c \tan \theta, \delta N_c \tan \theta, \epsilon N_c, \delta(N_a + N_c)] \cdot$$

$$\begin{bmatrix} T & 0 \\ 0 & T \end{bmatrix}^j \cdot \begin{bmatrix} N_c \tan \theta \\ N_c \tan \theta \\ N_c \\ N_a + N_c \end{bmatrix} \quad (23)$$

In eq 23, it has become necessary to employ a  $4 \times 4$  generator matrix, treating separately the  $x$  and  $z$  components of  $\mathbf{V}_0$  and  $\mathbf{V}_j$ . With the above modifications, eq 4 and 17 still apply, and we finally obtain

$$C_\infty = (1/3)[2x_a + (1 + x_c^2 \tan^2 \theta)x_a^{-1}] \quad (24)$$

Note that eq 24 becomes equivalent to eq 20 when  $\theta = 0$ , as expected.

The tilt tends to shift  $C_\infty$  to larger values, but the effect is not too strong, as seen in Figure 3. Even when  $\theta = 40^\circ$  one must go to crystallinities in excess of about 50% to see semicrystalline dimensions more than 10% above the molten dimensions.

In arriving at eq 24 we assumed that the chains in each lamella were inclined in precisely the same direction. This is probably not accurate. One could, of course, compute characteristic ratios for other tilt geometries, but we should not expect any qualitative differences from the present model.

### Anisotropy of the Distribution

If we carefully trace the development of terms in eq 20, we notice that the  $2x_a/3$  term results from displacements in the lamellar plane ( $x_a/3$  for each of the two degrees of freedom in the plane) while the  $(3x_a)^{-1}$  results from displacements normal to the plane. It follows that the end-to-end vector distribution function is anisotropic. Regions of constant probability are ellipsoids with semimajor axes proportional to  $x_a^{-1/2}$ , semiminor axes proportional to  $x_a^{1/2}$ , and aspect ratios equal to  $x_a^{-1}$ . The relationship  $\langle R_g^2 \rangle = \langle R^2 \rangle/6$  holds in spite of the anisotropy, so that eq 20 applies to the gyration radius as well as the end-to-end distance. This anisotropy is not immediately apparent from neutron scattering, since in polycrystalline samples all orientations of the lamellar plane occur with equal probability. Calculations are currently under way to de-

termine to what degree the anisotropy becomes apparent at higher scattering angles.

### Summary and Discussion

This calculation demonstrates the degree to which structures can be ordered and still conform to eq 1. With  $1/3$  random reentry, enough disorder is present for the development of Gaussian statistics. Bonds  $i$  and  $j$  are uncorrelated for most values of  $i$  and  $j$ . The bond correlations, when properly summed, yield the characteristic ratio. The correlation range is longer in the semicrystalline state, but an appreciable fraction of these correlations are negative, since loops reverse the chain direction. Then it is not surprising that these sum to give a characteristic ratio close to the value in the melt. Equations 20 and 24 indicate that the characteristic ratio is actually lower for small crystallinities. In the limit of very thin lamellae separated by thick amorphous layers, we expect a characteristic ratio very close to the melt value, but smaller, since the chains are turned back upon themselves.

A qualitative explanation for the small change in characteristic ratio is that the chains resist long-range reorganization during quench crystallization. Phrases such as "freezing in" are often employed, implying that the chains have the same global structure before and after solidification with no detectable differences at low resolution. Yet it appears that long-range reorganization must occur, since the chains assume an anisotropic distribution after crystallization. In any case, one need not assume absence of long-range reorganization to explain the small change in  $C_\infty$ .

Some comment on the range of applicability of the present model is in order. To avoid segregation, the neutron scattering experiments are performed on quench-crystallized samples. The result is a relatively low crystallinity (never much larger than 0.5 or 0.6). Implicit in this derivation is the assumption that different amorphous runs are uncorrelated, which is undoubtedly adequate for low-temperature, regime III crystallization.<sup>17</sup> We have also assumed  $2/3$  near-adjacent reentry,<sup>7</sup> but we

expect a higher degree of adjacent reentry for crystallization at higher temperatures. Therefore, the present model is probably not valid in all situations. This may explain the failure of isotactic polystyrene<sup>6</sup> to follow eq 1. Segregation effects are absent<sup>6</sup> in this polymer, and the measurements were performed on samples crystallized closer to the melting point.

### References and Notes

- (1) Schelten, J.; Ballard, D.; Wignall, G.; Longman, G.; Schmatz, W. *Polymer* **1976**, *17*, 751.
- (2) Ballard, D.; Cheshire, P.; Longman, G.; Schelten, J. *Polymer* **1978**, *19*, 379.
- (3) Fischer, E. W. *Pure Appl. Chem.* **1978**, *50*, 1319.
- (4) Crist, B.; Graessley, W. W.; Wignall, G. D. *Polymer* **1982**, *23*, 1561.
- (5) Tanzer, J. D.; Bartels, C. R.; Crist, B.; Graessley, W. W. *Macromolecules* **1984**, *17*, 2708.
- (6) Guenet, J. M.; Picot, C.; Benoit, H. *Faraday Discuss. Chem. Soc.* **1979**, *68*, 251.
- (7) Guttman, C. M.; DiMarzio, E. A.; Hoffman, J. D. *Polymer* **1981**, *22*, 1466.
- (8) Guttman, C. M.; DiMarzio, E. A. *Macromolecules* **1982**, *15*, 525.
- (9) Mansfield, M. L. *Macromolecules* **1983**, *16*, 914.
- (10) Flory, P. J.; Yoon, D. Y.; Dill, K. A. *Macromolecules* **1984**, *17*, 862.
- (11) Yoon, D. Y.; Flory, P. J. *Macromolecules* **1984**, *17*, 868.
- (12) Leermakers, F. A. M.; Scheutjens, J. M. H. M.; Gaylord, R. J. *Polymer* **1984**, *25*, 1577.
- (13) Ballard, D. G. H.; Burgess, A. N.; Crowley, T. L.; Longman, G. W.; Schelten, J. *Faraday Discuss. Chem. Soc.* **1979**, *68*, 279.
- (14) Guttman, C. M.; Hoffman, J. D.; DiMarzio, E. A., *Faraday Discuss. Chem. Soc.* **1979**, *68*, 297.
- (15) The argument for this is identical with the usual arguments relating different ensembles in the thermodynamic limit. The distribution of  $N$  becomes more sharply peaked as  $N$  increases.
- (16) Flory, P. J. "Statistical Mechanics of Chain Molecules"; Wiley: New York, 1969.
- (17) Equation 21 may be obtained as follows: Let  $\langle M \rangle_{\text{loop}}$  and  $\langle M \rangle_{\text{tie}}$  be the number of bonds in a loop (either adjacent or random) and a tie, respectively. Then

$$\langle N \rangle = n(N_c \sec \theta + \epsilon \langle M \rangle_{\text{loop}} + \delta \langle M \rangle_{\text{tie}})$$

$$\langle M \rangle_{\text{loop}} = (\sec \theta)/3 \text{ (the probability that a loop is random) times the average length of a random loop, } 2N_a \text{ (ref 7). } \langle M \rangle_{\text{tie}} \text{ is } N^2 \text{ (ref 7).}$$

- (17) Hoffman, J. D. *Polymer* **1983**, *24*, 3.

## Broken Wormlike Chain Model of Semiflexible Polymers

Marc L. Mansfield\*

Engineering Materials Program, Department of Chemical and Nuclear Engineering, University of Maryland, College Park, Maryland 20742. Received August 2, 1985

**ABSTRACT:** Traditionally, the flexibility of semiflexible polymers has been explained in one of two ways, either in terms of relatively small rotational angle fluctuations giving a smoothly bending curve or in terms of abrupt breaks, or kinks, in the chain. The original wormlike chain explicitly treats only the first of these two possibilities. Here we introduce the broken wormlike chain model, which explicitly incorporates both types of flexibility by inserting breaks at random intervals into the original wormlike chain, either through a fixed angle or through a universal joint. Exact expressions for the first three even moments and the radius of gyration are derived, and the hydrodynamic radius and static structure factor are approximated. We report very little difference between properties of broken and regular wormlike chains of the same total contour length and persistence length, which implies (1) that the original wormlike chain model provides an adequate description of most experiments independent of the nature of the flexibility and (2) that it may be difficult to determine experimentally which source of flexibility is operating in any given polymer.

### Introduction

A number of polymer chains, e.g., the poly(alkyl isocyanates)<sup>1-3</sup> or the DNA double helix,<sup>4-7</sup> are semiflexible, with rigid rod behavior at low molecular weights and

random coil behavior at high molecular weights. The Kratky-Porod or wormlike chain model<sup>8-11</sup> represents a semiflexible molecule as a smoothly bending space curve characterized by two parameters,  $L$ , the contour length of the curve, and  $\lambda$ , the stiffness parameter, having units of reciprocal length.  $(2\lambda)^{-1}$  is the correlation length or persistence length of the curve, the length over which directional correlation persists. Then the quantity  $L\lambda$  is pro-

\* Present address: Michigan Molecular Institute, Midland, MI 48640.